Rare Metal Materials and Engineering
Volume 52, Issue 3, March 2023
Available online at www.rmme.ac.cn

Science Press

Cite this article as: Li Chao, Shuang Yuanhua, Chen Chen, et al. Temperature Field Simulation of Titanium Alloy Seamless Pipe in Hot Continuous Rolling[J]. Rare Metal Materials and Engineering, 2023, 52(03): 791-797.

ARTICLE

Temperature Field Simulation of Titanium Alloy Seamless Pipe in Hot Continuous Rolling

Li Chao, Shuang Yuanhua, Chen Chen, Zhou Yan, Wang Chen, Mu Jiahao, Zhang Jian

Heavy Machinery Engineering Research Center, Ministry of Education, Taiyuan University of Science and Technology, Taiyuan 030024, China

Abstract: The finite element method was adopted to analyze the temperature state of titanium alloy seamless pipe during the multi-stand continuous rolling. The simulation results show that with increasing the rolling passes, the outer surface temperature under the groove vertex is decreased at a gradually reducing rate, the center temperature is basically increased at a gradually reducing rate, and the outer surface temperature under the groove taper is continuously increased. The circumferential unevenness of center temperature is decreased in odd passes and increased in even passes. However, the unevenness of temperature distribution on the outer surface has opposite variation trend. The rolling reduction of the front pass shows a negative correlation with temperature rise at the groove taper of the next pass. In addition, decreasing the rolling reduction of the former pass can significantly improve the circumferential temperature unevenness of the next pass. The results of temperature measurement and grain morphology show that the simulation results are in good agreement with the experiment results.

Key words: titanium alloy; seamless pipe; hot continuous-rolling; distribution of temperature field

With the development of oil and gas exploration in deep water and other extraordinary environments, such as high temperature, high pressure, and high corrosion, the new oil country tubular good materials with strong corrosion resistance and high performance are extensively required[1–3]. Therefore, titanium alloys become the attractive materials for oil country tubular good and offshore components due to their high specific strength, excellent corrosion resistance, long fatigue life, and outstanding mechanical properties in harsh environments[4–5].

Among various processes of titanium alloy pipe productions (forging, extrusion, cross piercing+cold rolling, and cross piercing+cross rolling+sizing), hot continuous rolling process has the advantages of multiple scale production, high production efficiency, low energy consumption, and short process[6]. For hot rolling treatment, rolling temperature is essential.

Technically, the accurate control of rolling temperature in hot rolling production plays a key role in achieving the breakthrough for the production of titanium alloy tubes. Since titanium alloy is sensitive to temperature due to its low thermal conductivity and high heat capacity, the local heat may easily occur in the process of material deformation[7]. In $\alpha+\beta$ titanium alloys, the α phase possesses a dense hexagonal structure, which affects the ductility and formability during rolling process. Raising deformation temperature can increase the β phase content and improve the deformation plasticity[8]. However, an excessively high temperature can exacerbate the coarsening of β grains, which significantly reduces the rolling properties[9]. Therefore, it is crucial to determine the temperature distribution in the deformation zone, which can significantly improve the mechanical properties of the products[10].

The temperature distribution in the seamless tube during the rolling process has been widely studied. Wang et al[11] investigated the temperature distribution of 45# steel tube during rolling by the three-dimensional elastic-plastic finite element method. Zhou et al[12] concluded that the temperature of 20# steel tube is most unevenly distributed along the thickness at the pass section. Dai et al[13] analyzed the

Received date: June 05, 2022
Foundation item: Major Science and Technology Projects of Shanxi Province (20191102009); Key R&D Projects of Shanxi Province (201903D121049); Basic Research Program of Shanxi Province (20210302123275)
Corresponding author: Shuang Yuanhua, Ph. D., Professor, Heavy Machinery Engineering Research Center, Ministry of Education, Taiyuan University of Science and Technology, Taiyuan 030024, P. R. China, Tel: 0086-351-2776763, E-mail: yhshuang@tyust.edu.cn

temperature distribution of AZ31 alloy pipes between the groove vertex and groove taper on the outer surface during the single stand rolling. Shi et al[14] studied the hot continuous rolling of TC4 alloy pipes and concluded that the best starting rolling temperature is 900–950 °C. Up to now, the researches on the circumferential distribution of pipe temperature during rolling process have rarely been conducted. Therefore, the hot continuous rolling process of titanium alloy seamless pipe was studied in this research to reveal the mechanism of uneven temperature distribution along the circumferential direction of titanium alloy pipes during hot continuous rolling. The relationship between uneven temperature and uneven strain was established to achieve the accurate control of temperature in the industrial-scale rolling process.

1 Strain Distribution of Pipe in Continuous Rolling

Although the single-stand tube rolling can be regarded as the rolling of a driving roller and an idle roller (mandrel), the strain distribution in this process is different from the flat rolling, as shown in Fig. 1. The rolling deformation zone can be divided into four parts. Among them, two parts are the direct deformation zones under the compression between the roller and the mandrel with different circumferential strains on the inner wall. These two parts are largely attributed to the circumferential flow of metal caused by the oval groove. Other two parts are the indirect deformation zones: one is that the outer wall and roller are in contact and the inner wall is away from the mandrel; the other is that neither the roller nor the mandrel is in contact with the pipe. Therefore, the metal flow is generated only by the bending constraint of the groove. As a result, the circumferential strain of the outer wall and the radial strain of the inner wall are close to zero, and the inner wall presents a significant circumferential strain.

Due to the non-uniformity of the strain at the groove vertex and the groove taper, the non-uniform temperature distribution is inevitable. Besides, the characteristics of multi-stand continuous rolling may cause more significant non-uniformity.

2 Finite Element Simulation Method

2.1 Finite element model

The hot continuous rolling model of TC4 hollow tube was established by DEFORM software, and Premium Quality Finishing (PQF) tandem mills were applied as the rolling equipment. The schematic diagram of finite element model is shown in Fig.2a, and the tube blank size was Φ160 mm×20.5 mm. Fig.2b shows the position of the characteristic nodes: P1–P7 represent the nodes with angle of 0°, 10°, 20°, 30°, 40°, 50°, and 60° at the center area, respectively; P8–P14 represent the nodes with angle of 0°, 10°, 20°, 30°, 40°, 50°, and 60° at the outer surface, respectively. Due to the symmetry of the model, only 1/6 of the model was used for the finite element simulation.

The heat transfer coefficient between the tube and roller was 20 MW·mm^{-2}·K^{-1}, and that between the thermal convection and thermal radiation was 0.15 MW·mm^{-2}·K^{-1} [14]. The heat conversion coefficient caused by friction and plastic deformation was 0.7 and 0.9, respectively[15–16], and the friction coefficient between the roller and tube was 0.3. Since the mandrel surface was coated by lubricant, the friction coefficient between the mandrel and pipe was 0.08[17–18].

2.2 Constitutive model

Because the rolling temperature, strain, and strain rate have significant influence on the rolling stress, the strain-compensated Arrhenius constitutive model[19] was used in this research, as follows:

$$Z = \dot{\varepsilon}\exp\left(\frac{Q}{RT}\right) \tag{1}$$

$$\sigma = \frac{1}{\alpha}\ln\left\{\left(\frac{Z}{A}\right)^{1/n} + \left[\left(\frac{Z}{A}\right)^{2/n}\right]^{1/2}\right\} \tag{2}$$

where Z represents the Zener-Hollomon parameter; Q refers to the activation energy of thermal deformation; T denotes the absolute temperature; R stands for the ideal gas constant; $\dot{\varepsilon}$ represents the true strain rate; σ denotes the true stress; α, n,

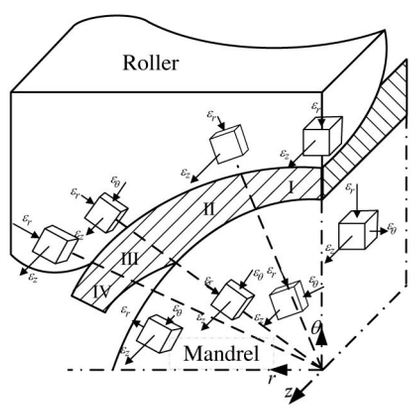

Fig.1 Strain states at rolling deformation zone in titanium alloy pipe

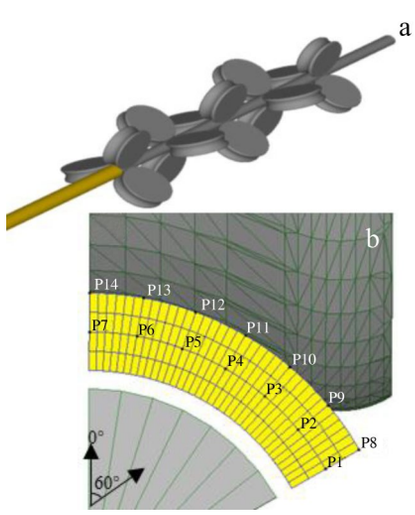

Fig.2 Schematic diagrams of finite element model for tube rolling (a) and the position of characteristic nodes (b)

and A are the material constants.

Table 1 shows the appropriate continuous rolling process parameters of titanium alloy pipes for finite element simulation.

3 Results and Discussion

3.1 Effective stress and nodal heat during rolling process

Fig.3 shows the deformation states caused by the roller and mandrel onto the pipe after the 1st pass. When the pipe enters the roller, the deformation firstly reduces, and the plastic heat is barely generated in the deformation zone. When the inner wall of the pipe comes into contact with the mandrel, the wall reduction deformation occurs. As shown in Fig.3a and 3b, the nodal heat at the center of groove vertex increases sharply, and the effective stress distribution is similar to the nodal heat distribution. However, the nodal heat at the inner and outer surface of the groove vertex is negative due to the heat exchange with the roller and the mandrel. As shown in Fig.3c and 3d, for the groove taper, the nodal heat is positive, and the heat distribution is similar to the effective stress distribution. Therefore, the plastic heat generation is the main heating mechanism at the groove taper.

3.2 Rolling temperature field

Due to different processing parameters, each pass affects the pipe temperature in a different way. Fig. 4 shows the temperature distribution at cross section of the exit side of each pass. After the 1st pass, the ovality of the cross section of pipe is quite obvious, and the ear phenomenon at the groove taper is enhanced. In addition, the surface temperature drops to about 900 °C, while the center temperature rises to about 952 °C. After the 2nd pass, the ovality of the cross section of pipe is reduced, and the ear phenomenon at the groove taper is weakened, compared with those of the 1st pass. The temperature of the outer surface continuously reduces to 890 °C, and the center temperature at the groove vertex increases to 977 °C, which is far more than that of the 1st pass. At the same time, the center temperature of the groove taper rises to about 959 °C, which indicates that the temperature distribution between the groove vertex and groove taper is uneven. After the 3rd pass, the ovality of the cross section of pipe almost disappears, and the ear phenomenon is negligible. The temperature on the outer surface reaches the minimum of 878 °C, while the center temperature at the groove vertex rises to 965 °C, suggesting that the temperature rise at the groove taper is negligible. After the 4th pass, the pipe cross section is basically round, and the temperature reaches 985 °C at the center of the groove vertex, which is the maximum temperature during the rolling process. The temperature at the groove taper shows no significant change, whereas the center temperature increases slightly, compared with those of the previous pass. After the 5th pass, the cross section shape and temperature distribution are almost identical to those of the 4th pass.

With increasing the number of rolling passes, the temperature decreasing rate of the outer surface is reduced. This is because the heat transfer of the 1st and 2nd passes

Table 1 Continuous rolling process parameters of titanium alloy pipes for finite element simulation

Pass	1st	2nd	3rd	4th	5th
Distance between each stand/mm			780		
Distance between roller centerline and rolling centerline/mm	307.50	305.75	308.75	310.00	296.25
Mandrel diameter/mm			127		
Mandrel insert speed/m·s^{-1}			1.5		
Mandrel speed in rolling/m·s^{-1}			0.9		
Rotational speed of roller/r·min^{-1}	73	106	149	182	228
Rolling eccentricity/mm	15.23	12.47	7.92	3.74	0.00
Rolling radius/mm	74.60	71.15	69.20	68.40	68.40

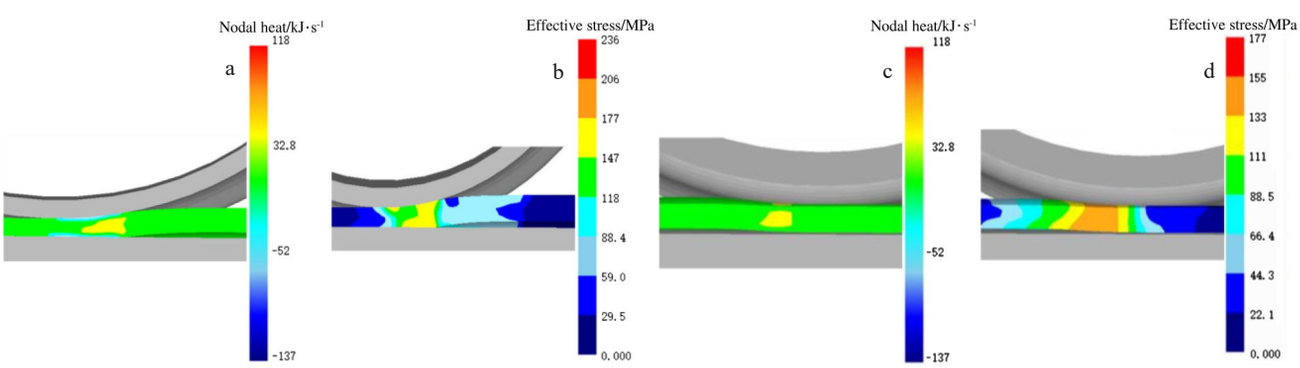

Fig.3 Nodal heats (a, c) and effective stresses (b, d) at groove vertex (a, b) and groove taper (c, d) of longitudinal section of tube after 1st pass of continuous rolling

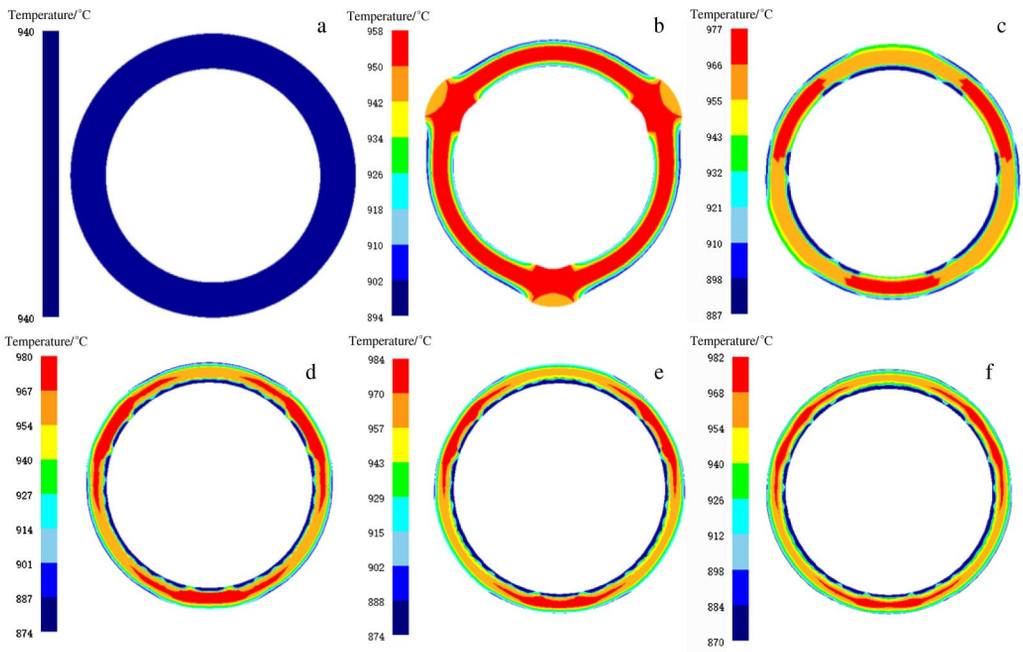

Fig.4 Temperature field distributions at cross section of pipe exit after each pass during continuous rolling: (a) initial, (b) 1st pass, (c) 2nd pass, (d) 3rd pass, (e) 4th pass, and (f) 5th pass

consumes plenty of heat, while the roller speed of the 3rd and 4th passes is high and the contact area is restricted, which gradually reduces the heat transferred by rollers. In addition, the core heat is also transferred to the outer surface through the internal heat. The temperature increasing rate at the center area decreases, which is largely attributed to the large deformation of pipe and the high plastic temperature in the early and middle stages of rolling. In the last two passes, when the deformation is insignificant, the heat is transferred to the inner and outer surfaces through the internal heat conduction, which slows the temperature growth trend.

Fig. 5a and 5b show the temperature changes of P1 – P7 nodes at the center area and P8 – P14 nodes at the outer surface, respectively. The center temperature fluctuates over time. During the 1st – 4th passes, the temperature increases, whereas it declines in the 5th pass. The change of surface temperature over time results from the alternation of cooling and heating. For the outer surface, the cooling and heating changes alternately in the groove vertex area, while the groove taper area is continuously heated. Moreover, the temperature gradient along the thickness direction increases firstly and then decreases during the rolling process. For a single pass, the maximum temperature difference occurs at the end of rolling contact, while the minimum temperature difference occurs at the beginning of the next pass. The main reason is that in the rolling contact stage, the temperature change is intensified by the contact heat transfer and plastic deformation heat energy. In the rolling disengagement stage, the temperature of the tube tends to stabilize by the heat conduction, which leads to the insignificant temperature difference.

In addition, the temperature distribution is non-uniform

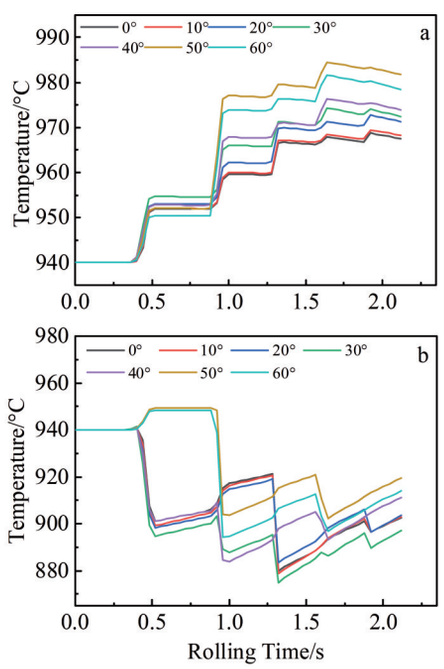

Fig.5 Temperature variations with rolling time at center area (a) and outer surface (b) of pipe during continuous rolling

along the circumference direction of the outer surface and the center area: the temperature at the center area shows a decreasing trend in odd passes and an increasing trend in even passes, resulting in a peak circumferential temperature difference of about 20 °C in the 2nd pass. However, the temperature at the outer surface shows an increasing trend in odd passes but a decreasing trend in even passes. The peak temperature difference of the outer surface occurs in the 1st

pass, which reaches about 55 °C, and the lowest temperature is 878 °C after the 3rd pass of rolling.

The non-uniformity of the circumferential deformation in the 2nd pass leads to the peak temperature difference. The large reduction at the groove vertex after the 2nd pass results in the significant temperature rise at the groove vertex, compared with that after the 1st pass. The less significant temperature rise at the groove taper mainly results from the gradual decrease in the ovality of the groove, which affects the circumferential strain. Meanwhile, the shrinkage ratio of the cross section area also reduces gradually, which affects the axial strain. These phenomena all restrict the strain at the groove taper. Meanwhile, the plastic heat generation shows that the strain has an effect on the node temperature[20].

Based on the fact that the direct deformation zones only contribute to a minor longitudinal shift which is relative to the indirect deformation zones in the deformation process[21], the axial strain can be neglected for the analysis of circumferential temperature difference. Despite the large radial strain at the groove vertex, the difference in temperature distributions between the 1st pass and the 2nd pass is caused by the significant circumferential strain, which results from the ear phenomenon at the groove taper and leads to a relatively uniform temperature distribution between the groove vertex and groove taper of the 1st pass. For the 2nd pass, the radial strain at the groove vertex is greater than the circumferential strain at the groove taper due to the unevenness of deformation.

3.3 Effect of rolling reduction on circumferential temperature unevenness

The reduction ratios of 10%, 20%, 30%, 40%, and 50% for the 1st pass were selected to simulate the change in center temperature during the 2nd pass, and the rolling reduction of the 2nd pass was unchanged. Fig. 6a shows the temperature changes of P1 – P7 nodes in the 1st pass under different reduction ratios, and Fig.6b shows the temperature changes of P1 – P7 nodes in the 2nd pass. It can be seen that the center temperature in the 1st pass is increased with increasing the reduction ratio, presenting the uniform distribution along the circumference direction. The increase in the reduction ratio of the 1st pass not only increases the center temperature of the 2nd pass, but also exacerbates the uneven circumferential temperature distribution in the center area of the 2nd pass. As shown in Fig. 6c, the increase in the reduction ratio of the 1st pass reduces the temperature increment at the groove taper of the 2nd pass, despite that the temperature rise at the groove vertex is not affected. This phenomenon results from the significant rolling reduction of the 1st pass, which decreases the effect of the 2nd pass at the groove taper of pipe. Consequently, the circumferential strain and radial strain of pipe after the 2nd pass are basically unchanged, compared

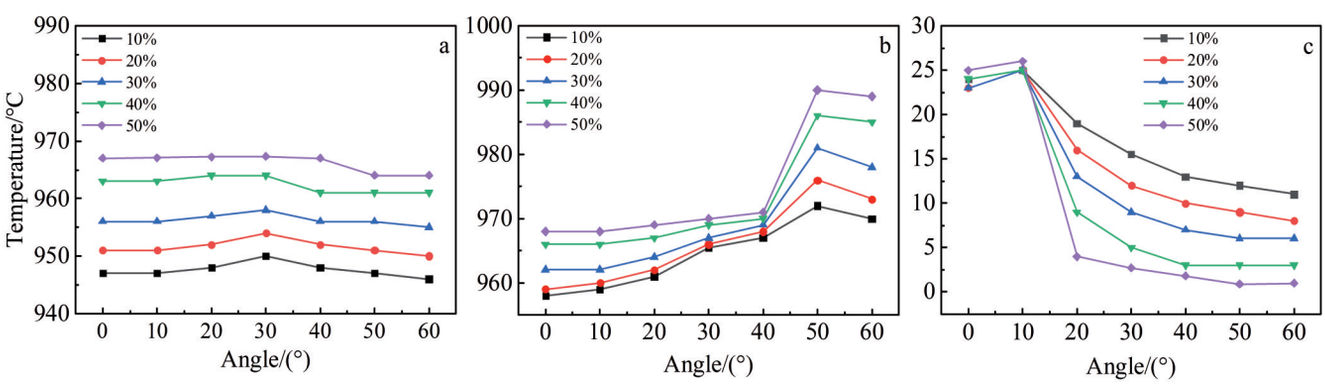

Fig.6 Center temperatures of pipe after the 1st pass (a) and the 2nd pass (b) under different reduction ratios of the 1st pass; center temperature differences between the 1st pass and the 2nd pass under different reduction ratios of the 1st pass (c)

with those of the 1st pass. As the uneven deformation between groove vertex and grove taper becomes more significant, the unevenness of circumferential temperature distribution is enhanced. It can also be seen from Fig. 7 that the change of circumferential strain under different reduction ratios of the 1st pass is positively correlated with the change of center temperature.

4 Experiment

To verify the accuracy of the simulation results, the experiments were conducted for the TC4 pipes with the initial temperature of 940 ° C. The microstructures at pipe center after different rolling passes are shown in Fig. 8. It can be found that the equiaxed *α* phase in the 2nd rolling pass is less

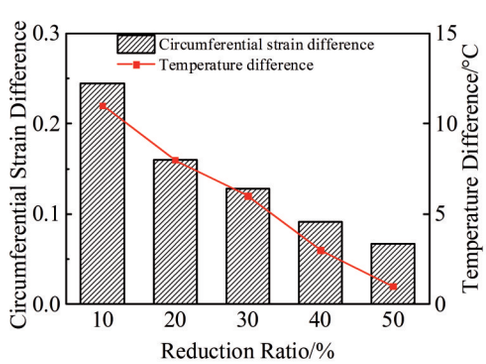

Fig.7 Relationships of circumferential strain difference and center temperature difference with different reduction ratios of the 1st pass

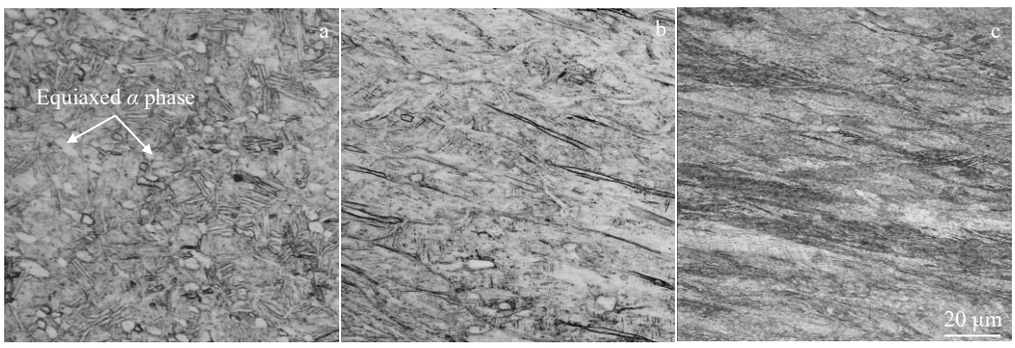

Fig.8 Microstructures of seamless pipe at initial state (a) and after continuous rolling for the 2nd pass (b) and the 4th pass (c)

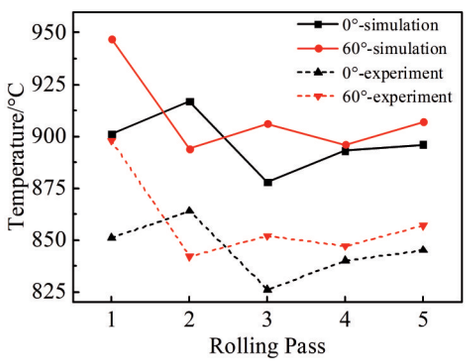

Fig.9 Experimental and simulated outer surface temperatures after each rolling pass

than that in the initial state, and there is even less equiaxed α phase in the 4th pass. Because the center temperature of the pipe continuously increases during the rolling process until it reaches the peak temperature after the 4th rolling pass, the equiaxed α phase is gradually dissolved into the β matrix. The experiment results are in good agreement with the simulation results.

Fig. 9 shows the temperature distributions on the outer surface of titanium alloy pipe during the rolling process. The infrared thermometer was set at the positions with an angle of 0° and 60° at the outlet for comparison with the simulation results. It can be found that the variation trends of simulation results agree well with those of the experiment results. However, the experiment results are significantly lower than the calculation results. This is due to the heat exchange with the roller table and the surrounding environment before the tube enters the rolling mill. Therefore, the actual rolling temperature is lower than 940 °C, which leads to the relatively lower measured temperatures. Briefly, because the temperature rise at the center of titanium alloy pipe during hot rolling is significant, overheating can be controlled by improving the groove, reducing the deformation, and reducing the rolling speed. Thus, the grain coarsening can also be prevented.

5 Conclusions

1) With increasing the rolling passes, the outer surface temperature under the groove vertex is decreased at a gradually reducing rate, the center temperature is basically increased at a gradually reducing rate, and the outer surface temperature under the groove taper is continuously increased. Because the temperature rise at the center of titanium alloy pipe during hot rolling is significant, overheating can be controlled by improving the groove, reducing the deformation, and reducing the rolling speed. Thus, the grain coarsening can also be prevented.

2) During the rolling process, the uneven temperature distributions along the circumferential direction occur on both the center and the outer surface of pipe. The temperature at the center area shows a decreasing trend in odd passes and an increasing trend in even passes, whereas the temperature at the outer surface shows an increasing trend in odd passes but a decreasing trend in even passes.

3) By changing the rolling reduction of the 1st pass, the unevenness of circumferential temperature distribution caused by uneven deformation can be reduced by increasing the circumferential strain at the groove taper and increasing the temperature rise. Therefore, the uneven circumferential temperature distribution is reduced and the uniformity of microstructure is improved.

References

1 Shadravan A, Amani M. *Energy Science and Technology*[J], 2012, 4(2): 36

2 Du Wei, Li Helin. *Petroleum Tubular Goods & Instruments*[J], 2015, 1(5): 1 (in Chinese)

3 Zhang Shuichang, Zhang Baomin, Li Benliang *et al*. *Petroleum Exploration and Development*[J], 2011, 38(1): 1 (in Chinese)

4 Schutz R W, Watkins H B. *Materials Science and Engineering A*[J], 1998, 243(1–2): 305

5 Boyer R R. *Materials Science and Engineering A*[J], 1996, 213(1–2): 103

6 Wang Chaofeng, Xue Jianguo, Zhou Zhiyang *et al*. *Non-Ferrous Mining and Metallurgy*[J], 2015, 31(4): 34 (in Chinese)

7 Warchomicka F, Stockinger M, Degischer H P. *Journal of Materials Processing Technology*[J], 2006, 177(1–3): 473

8 Li Junzhao, Sun Qingjie, Yu Hang. *Iron Steel Vanadium Tita-*

nium[J], 2021, 42(6): 17 (in Chinese)
9 Han Chunhui. *Investigation on the Deformation Processing and Relationship Between Microstructure and Property of TC4 Alloy Ring Part*[D]. Harbin: Harbin Institute of Technology, 2015 (in Chinese)
10 Mulyadi M, Rist M A, Edwards L *et al*. *Journal of Materials Processing Technology*[J], 2006, 177(1–3): 311
11 Wang F X, Du F S, Yu H. *Advanced Materials Research*[J], 2011, 189: 1670
12 Zhou Yan. *Key Technology and Characteristic Study of the Continual Mandrel Rolling Compact Process for Producing Minor Diameter Seamless Steel Tubes*[D]. Taiyuan: Taiyuan University of Science and Technology, 2016 (in Chinese)
13 Dai Jia. *Experimental Study on Longitudinal Continuous Rolling Technology of Magnesium Alloy Pipe*[D]. Taiyuan: Taiyuan University of Science and Technology, 2020 (in Chinese)
14 Shi J X, Yu W, Dong E T *et al*. *Advances in Materials Processing: Proceedings of Chinese Materials Conference 2017*[C]. Singapore: Springer, 2017: 705
15 Nemat-Nasser S, Guo W G, Nesterenko V F *et al*. *Mechanics of Materials*[J], 2001, 33(8): 425
16 Yoshida M. *AIP Conference Proceedings*[C]. Bolu: American Institute of Physics, 2010, 1252(1): 1333
17 Takahashi K, Inoue T, Uchida S. *Nippon Steel Technical Report*[J], 2002(85): 41
18 Wang Haidou, Xu Binshi, Liu Jiajun. *Micro and Nano Sulfide Solid Lubrication*[M]. Beijing: Science Press, 2011 (in Chinese)
19 Hu Ming, Dong Limin, Zhang Zhiqiang *et al*. *Rare Metal Materials and Engineering*[J], 2020, 49(3): 956 (in Chinese)
20 Khan A S, Suh Y S, Kazmi R. *International Journal of Plasticity*[J], 2004, 20(12): 2233
21 Sobkowiak P. *Journal of Materials Processing Technology*[J], 1996, 61(4): 347

钛合金无缝管热连轧温度场模拟

李　潮，双远华，陈　晨，周　研，王　琛，穆佳浩，张　坚
(太原科技大学 重型机械教育部工程研究中心，山西 太原 030024)

摘　要：采用有限元法分析了钛合金无缝管多机架连轧下的温度状态。模拟结果表明：随轧制道次的增加，辊底下的外表面温度以逐渐减缓的速率降低，中心温度整体上以逐渐减缓的速率上升，而辊缝下外表面温度持续升高。中心温度的周向不均匀性在奇数道次时减小，在偶数道次时增大，而外表面温度分布的不均匀性与此相反。前一机架压下量与后机架辊缝处温升呈负相关，降低前一机架压下量可显著提升后机架周向温度不均匀性。温度测量和晶粒形貌分析的结果表明，模拟结果与实验结果吻合度较高。

关键词：钛合金；无缝管；热连轧；温度场分布

作者简介：李　潮，男，1994年生，博士生，太原科技大学重型机械教育部工程研究中心，山西 太原 030024，电话：0351-2776769，E-mail：B20190011@stu.tyust.edu.cn